An analytical formula for fluctuations in nuclear charge density

A. R. Abdulghany

Physics Department, Faculty of Science, Cairo University, Giza, Egypt

Abstract: The experimental charge densities of atomic nuclei show fluctuations in their distributions. This paper investigates the limits of accuracy of two-parameter Fermi and three-parameter Fermi distributions in describing the charge density. An improved analytical function for density distribution is proposed, which allows for density fluctuation. The experimental charge densities of ^{40}Ca, ^{60}Ni, ^{100}Mo, ^{152}Sm and ^{208}Pb, representing the various shapes of density fluctuation, are used to assess the accuracy of the proposed formula. The proposed function reproduces the experimental charge densities with significant improvement in accuracy over other commonly used formulae. A compilation of charge density distribution parameters of 73 nuclei is presented based on the proposed formula.

Keywords: nuclear density, density-fluctuation, Fermi distribution function

PACS: 21.10.Ft, 21.10.Gv **DOI:** 10.1088/1674-1137/42/7/074101

1 Introduction

In the 1950s, Hofstadter and collaborators used electron scattering to characterize the charge distribution of nucleons and nuclei [1]. From the cross-section ($\mathrm{d}\sigma/\mathrm{d}\Omega$) of the electron scattering, the form factor $F(k)$ can be deduced. Furthermore, the charge densities $\rho(r)$ can be produced in the form of model-independent distributions, such as the Fourier-Bessel expansion [2–4], or further simplified to analytical formulae [2–5]:

$$\frac{\mathrm{d}\sigma}{\mathrm{d}\Omega}\xrightarrow[\text{correction}]{\text{Coulomb}}F(k)\xrightarrow[\text{transform.}]{\text{Fourier}}\rho(r)\xrightarrow[\text{formula}]{\text{fitting to}}\text{parameters.}$$

The two-parameter Fermi (2pF) function is always considered as an acceptable approximation of the charge, proton, and neutron distributions [6–8]. The 2pF function is given by Eq. (1),

$$\rho(r)=\frac{\rho_0}{1+\mathrm{e}^{(r-R)/a}}, \tag{1}$$

where a is the diffuseness parameter and R is the radius parameter. The central density ρ_0 is determined by the normalization to the number of protons (Z) or neutrons (N).

A common alternative to the 2pF function is the three-parameter Fermi function (3pF), given by Eq. (2), where a central depression parameter (w) is introduced:

$$\rho(r)=\frac{\rho_0[1+w(r^2/R^2)]}{1+\mathrm{e}^{(r-R)/a}}. \tag{2}$$

The central depression parameter allows the central density to be depressed or raised, depending on the sign of w. The 2pF function is the most widely used analytical formula in the study of nuclear structure, nuclear reactions, alpha decay and cluster decay [6, 8–13]. Although the 2pF function gives acceptable results, using the 3pF distribution improves the binding energy calculation, especially for superheavy and ultraheavy regions, as the ground state has a depression in the central density[14]. Moreover, the calculation of alpha decay half-life and preformation probability is very sensitive to the central depression parameter [15]. In a recent study of ^{208}Pb charge density, Jones et al. compared the two formulae to each other [7]. The study showed that the fitting of model-independent data to the 3pF distribution does not provide a significant improvement over the fitting to 2pF. The present work shows that the 3pF function provides a reasonable improvement for some nuclei over the case of ^{208}Pb.

In fact, using model-independent analysis of electron scattering, the fluctuating character of the charge density was evident. The shell model and self-consistent analysis also show such fluctuations in the proton and neutron densities [16–18]. The 2pF function and 3pF function both show smooth variation without any fluctuation at all. The fitting of the model-independent data to both functions is quite good at the tail of the distribution, but the situation is different at the core, at which the fluctuations exist. The purpose of the present work is to propose an improved formula to describe density fluctuations at the nucleus interior.

Received 20 February 2018, Revised 12 April 2018, Published online 18 May 2018

1) E-mail: abdulghany@sci.cu.edu.eg

2 Improved density fluctuation formula

Let us call the new function "double 3pF (d3pF)", since it is composed of two 3pF parts, one with a large radius parameter, which describes the tail of the distribution, and the second with a smaller radius, which describes the density fluctuation in the vicinity of the center.

The d3pF function is given by Eq, (3), where the δ_i's are the weights of the two 3pF parts:

$$\rho(r)=\rho_0\sum_{i=1,2}\frac{\delta_i[1+w_i(r^2/R_i^2)]}{1+\mathrm{e}^{(r-R_i)/a_i}}, \tag{3}$$

$$\delta_2=1-\delta_1.$$

This function has seven independent parameters, since the density distribution should verify the normalization condition.

3 Results and discussion

In the present work, the experimental charge densities of ^{40}Ca, ^{60}Ni, ^{100}Mo, ^{152}Sm, and ^{208}Pb were used to assess the ability of the aforementioned formulae to describe the nucleon density. Regardless of the position of the nuclide in the chart of nuclides, this study is concerned with the quality of fitting. For this purpose, this study focused on five different shapes of density distribution, which represent the common shapes of density fluctuation.

The main results of the study are summarized in Fig. 1. The left-hand panels show the model-independent distributions of ^{40}Ca, ^{60}Ni, ^{100}Mo, ^{152}Sm, and ^{208}Pb with the corresponding fitted 2pF, 3pF, and d3pF distributions. The right-hand panels of Fig. 1 show the residuals of the fits of the corresponding left-hand panels. In addition to the residuals, there are three bars on each right-hand panel, showing the difference between the highest and lowest values of residual for the three formulae. It is clear that 2pF and 3pF reproduce the model-independent density with appropriate accuracy, except for the interior fluctuation. As seen in Fig. 1, the d3pF distribution has two advantages over the other two distributions. The first advantage is that it reproduces the model-independent density with much higher overall accuracy. The second advantage is that it allows for fluctuation in density, which can be adjusted to match the actual fluctuation.

Contrary to expectations, the difference between the highest and lowest values of residual for 3pF distribution is not always smaller than its value for 2pF distribution, moreover, it could be greater. For ^{60}Ni and ^{208}Pb, it is obvious that the length of the bar representing the difference between residual extremes for the 3pF distribution is greater than the adjacent bar, corresponding to the 2pF distribution. The value of the residual extreme is not sufficient to indicate the goodness of fit, but it is still important since it indicates how the expected value is far from the real value at the worst point. In assessing the goodness of the fit, the residual sum of squares (RSS) is calculated for the three formulae considered in this study. The values of RSS are presented in Table 1

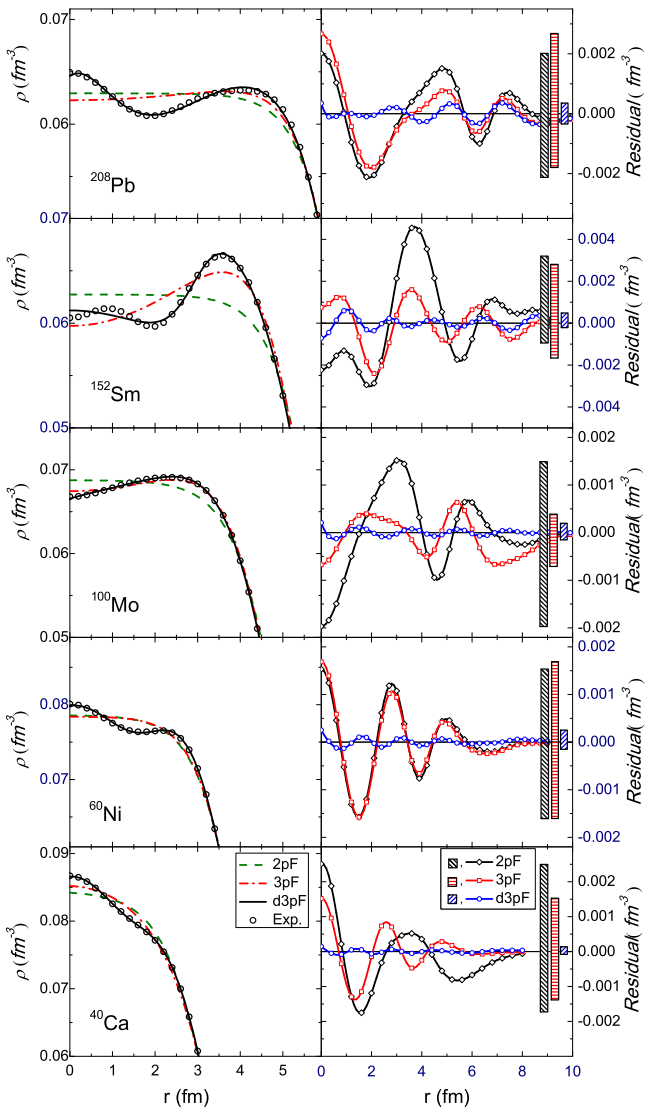

Fig. 1. (color online) The left-hand panels show the model-independent distributions (circles) of ^{40}Ca, ^{60}Ni, ^{100}Mo, ^{152}Sm, and ^{208}Pb, respectively, from bottom to top, with the corresponding fitted 2pF (green dashed line), 3pF (red dash-dotted line), and d3pF (black line) distributions. The right-hand panels show the residuals of the fits of the corresponding left-hand panels. The three bars on each right-hand panel represent the difference between the highest and lowest values of residual. The bars correspond to 2pF, 3pF and d3pF distributions respectively, from left to right.

Table 1. Density distribution parameters obtained from the fitting of model-independent density to 2pF, 3pF, and d3pF distributions, in addition to the residual sum of squares (RSS) for each distribution. The two rows corresponding to d3pF represent the two parts of the distribution; the first row is for parameters with $i=1$, and the second is for parameters with $i=2$, as defined in Eq. (3).

nucleus	model	R/fm	a/fm	w	δ	RSS
^{40}Ca	2pF	3.564	0.613			6.769E-5
	3pF	3.842	0.574	-0.211		2.792E-5
	d3pF	3.793	0.644	-0.279		1.706E-7
		1.506	0.479	0.927	-0.146	
^{60}Ni	2pF	4.179	0.548			4.210E-5
	3pF	4.156	0.553	0.021		4.139E-5
	d3pF	4.287	0.641	-0.300		4.245E-7
		1.903	0.524	0.544	-0.301	
^{100}Mo	2pF	5.054	0.582			6.582E-5
	3pF	4.852	0.633	0.167		1.569E-5
	d3pF	5.086	0.756	-0.283		3.718E-7
		4.008	1.158	-0.172	-0.981	
^{152}Sm	2pF	5.964	0.547			3.835E-4
	3pF	5.602	0.651	0.329		8.969E-5
	d3pF	5.997	0.652	-0.233		6.797E-6
		2.942	0.368	0.016	-0.261	
^{208}Pb	2pF	6.627	0.544			1.044E-4
	3pF	6.556	0.569	0.063		8.654E-5
	d3pF	6.577	0.594	-0.056		4.626E-6
		0.002	0.952	0.0	-0.189	

Table 2. d3pF density distribution parameters.

nucleus	^{3}H	^{3}He	^{12}C	^{15}N	^{16}O	^{26}Mg	^{27}Al
R_1	9.2436E-1	1.2673E0	2.2990E0	2.7561E0	2.8326E0	3.4404E0	3.2265E0
a_1	4.2671E-1	4.1269E-1	5.6181E-1	6.2397E-1	6.5983E-1	6.0467E-1	6.0983E-1
w_1	1.4417E-1	1.4120E-1	-1.6192E-1	-8.2719E-1	-6.4035E-1	-4.9772E-1	-2.5839E-1
R_2	7.9977E-1	7.7785E-1	8.4162E-1	7.5836E-1	7.2364E-1	1.9101E0	1.5738E0
a_2	4.1458E-1	3.7286E-1	4.3754E-1	7.2031E-1	7.5518E-1	6.2798E-1	5.2184E-1
w_2	2.3518E-1	1.1835E0	-1.1782E0	2.0910E0	4.1672E0	2.0090E0	-1.3537E0
δ_2	-4.8601E0	-6.2642E-1	-1.2073E-1	1.6880E-1	5.8846E-2	1.9797E-1	-1.4211E-1
RSS	5.3202E-7	1.1325E-6	6.1078E-8	7.0408E-7	4.0016E-7	3.3108E-7	1.7890E-7
$\chi^2_{\rm red}$	1.7162E-8	2.3594E-8	7.5405E-10	9.7788E-9	4.9402E-9	3.9889E-9	2.5558E-9
nucleus	^{28}Si	^{29}Si	^{30}Si	^{31}P	^{32}S	^{34}S	^{36}S
R_1	3.2791E0	2.4054E0	3.4365E0	3.6043E0	3.8429E0	3.5412E0	3.6135E0
a_1	6.2981E-1	7.2397E-1	5.7601E-1	5.4255E-1	4.9948E-1	6.3443E-1	6.0827E-1
w_1	-2.5744E-1	6.8221E-1	-1.7804E-1	-1.7989E-1	-1.1195E-1	-2.5044E-1	-2.5496E-1
R_2	1.3371E0	4.6807E0	2.3923E0	2.6410E0	3.2688E0	1.4529E0	1.0752E0
a_2	4.7401E-1	7.1594E-1	4.4523E-1	4.8274E-1	3.3521E-1	2.2516E-1	3.1194E-1
w_2	-1.9184E-1	4.5270E-1	1.1619E0	2.2667E-1	-7.3533E-1	1.2870E0	-6.8671E-1
δ_2	-1.5866E-1	-1.6771E-1	1.4749E-1	3.3908E-1	4.2682E-1	-7.3528E-3	4.0467E-2
RSS	1.2328E-7	7.9465E-6	6.1715E-8	4.3093E-8	1.1251E-6	2.5550E-7	1.4077E-7
$\chi^2_{\rm red}$	1.5035E-9	9.6908E-8	7.1762E-10	5.3201E-10	1.3890E-8	3.1543E-9	1.7168E-9

Continued on next page

Table 2 – continued from previous page

nucleus	^{40}Ar	^{40}Ca	^{48}Ca	^{48}Ti	^{50}Ti	^{50}Cr	^{52}Cr
R_1	3.8542E0	3.7935E0	3.9324E0	4.0691E0	3.8461E0	3.9308E0	4.1556E0
a_1	6.9361E-1	6.4417E-1	6.1175E-1	6.1848E-1	5.5560E-1	5.6192E-1	6.1102E-1
w_1	-3.4139E-1	-2.7905E-1	-3.2909E-1	-3.1206E-1	-2.4530E-2	1.6100E-3	-3.3312E-1
R_2	1.5842E0	1.5056E0	1.6584E0	1.8677E0	1.2644E0	1.0002E0	2.5496E0
a_2	5.1736E-1	4.7907E-1	4.7813E-1	3.9405E-1	2.8897E-1	2.0147E-1	3.0802E-1
w_2	-1.1291E0	9.2687E-1	7.1396E-1	5.8100E-2	-2.0719E0	-3.0566E0	-3.9192E-1
δ_2	-1.1778E-1	-1.4630E-1	-2.3476E-1	-1.4627E-1	4.2204E-2	-1.4764E-2	-2.1175E-1
RSS	1.6794E-6	1.7057E-7	3.4386E-7	6.8215E-7	5.8736E-6	4.6089E-6	1.0670E-6
$\chi^2_{\rm red}$	1.8255E-8	2.3365E-9	4.2452E-9	6.6229E-9	5.9329E-8	5.0097E-8	1.1598E-8
nucleus	^{54}Cr	^{54}Fe	^{56}Fe	^{58}Fe	^{59}Co	^{58}Ni	^{60}Ni
R_1	4.1766E0	4.2187E0	4.2553E0	4.3000E0	4.2783E0	4.2252E0	4.2869E0
a_1	6.1394E-1	6.1642E-1	6.2475E-1	6.6670E-1	6.6966E-1	6.1929E-1	6.4093E-1
w_1	-3.0085E-1	-3.2516E-1	-3.0819E-1	-3.4033E-1	-3.2123E-1	-2.7571E-1	-3.0043E-1
R_2	1.9165E0	1.8006E0	2.0590E0	1.7122E0	1.6742E0	1.8875E0	1.9032E0
a_2	4.5580E-1	4.8184E-1	4.8801E-1	4.8965E-1	5.1294E-1	5.1335E-1	5.2441E-1
w_2	2.6360E-1	4.5452E-1	4.9450E-2	6.8627E-1	8.7388E-1	5.2908E-1	5.4377E-1
δ_2	-1.8590E-1	-2.8344E-1	-2.4212E-1	-2.5105E-1	-2.8550E-1	-3.0937E-1	-3.0057E-1
RSS	3.6359E-7	6.9870E-7	2.6935E-7	7.6302E-7	8.3626E-7	4.6090E-7	4.2454E-7
$\chi^2_{\rm red}$	3.9521E-9	7.5946E-9	2.9277E-9	8.2937E-9	9.0898E-9	5.0098E-9	5.1149E-9
nucleus	^{62}Ni	^{64}Ni	^{63}Cu	^{65}Cu	^{64}Zn	^{66}Zn	^{68}Zn
R_1	4.4044E0	4.5188E0	4.3810E0	4.4369E0	4.4850E0	4.5048E0	4.5338E0
a_1	6.4913E-1	6.2448E-1	6.9416E-1	6.8446E-1	6.8209E-1	6.9578E-1	7.1244E-1
w_1	-3.4145E-1	-3.6240E-1	-3.2262E-1	-3.3263E-1	-3.3371E-1	-3.4630E-1	-3.6011E-1
R_2	1.9041E0	2.4867E0	1.7675E0	1.8314E0	2.4583E0	2.0531E0	1.8143E0
a_2	5.3294E-1	3.4551E-1	5.2957E-1	5.3683E-1	5.5500E-1	5.0694E-1	5.3965E-1
w_2	5.1774E-1	-2.1741E-1	7.5229E-1	7.1064E-1	-2.9786E-1	1.6236E-1	7.8381E-1
δ_2	-2.9597E-1	-2.3323E-1	-2.9280E-1	-2.9756E-1	-2.4255E-1	-2.5961E-1	-2.9229E-1
RSS	4.5775E-7	6.5075E-7	7.8547E-7	9.0185E-7	8.1040E-8	3.1537E-7	1.2787E-6
$\chi^2_{\rm red}$	4.9756E-9	7.0733E-9	8.5377E-9	9.8027E-9	8.8087E-10	3.4279E-9	1.3899E-8
nucleus	^{70}Zn	^{70}Ge	^{72}Ge	^{74}Ge	^{76}Ge	^{88}Sr	^{90}Zr
R_1	4.5350E0	4.5191E0	4.5830E0	4.7285E0	4.7553E0	4.7798E0	4.8298E0
a_1	7.2306E-1	7.7272E-1	7.7954E-1	6.7493E-1	6.6457E-1	6.2327E-1	5.7818E-1
w_1	-3.5686E-1	-3.4150E-1	-4.7618E-1	-3.3429E-1	-3.4364E-1	-7.6790E-2	3.9300E-3
R_2	1.7646E0	3.6747E0	3.7624E0	2.8898E0	2.8940E0	1.5598E0	7.2557E-1
a_2	5.3854E-1	1.0411E0	9.2562E-1	4.9041E-1	4.7732E-1	1.0944E0	3.2347E-1
w_2	9.1955E-1	-2.4447E-1	-4.7648E-1	-6.1329E-1	-5.3847E-1	2.1178E-1	1.5613E-1
δ_2	-3.2653E-1	-9.6409E-1	-1.0414E0	-1.9686E-1	-2.2732E-1	-4.2572E-1	-1.0144E-1
RSS	2.6089E-6	3.9632E-7	3.1906E-7	1.1335E-7	1.8819E-7	3.4562E-6	5.4645E-6
$\chi^2_{\rm red}$	2.8358E-8	3.8478E-9	3.0977E-9	1.1005E-9	1.8270E-9	3.7567E-8	5.3053E-8
nucleus	^{92}Zr	^{94}Zr	^{92}Mo	^{94}Mo	^{96}Mo	^{98}Mo	^{100}Mo
R_1	4.8635E0	4.9071E0	4.9145E0	4.9690E0	5.0203E0	5.1083E0	5.0862E0
a_1	5.9278E-1	6.0007E-1	5.7038E-1	5.8353E-1	5.9370E-1	6.6432E-1	7.5616E-1
w_1	-1.3140E-2	-4.3340E-2	-1.4850E-2	-5.3640E-2	-8.5350E-2	-2.1238E-1	-2.8296E-1
R_2	7.8755E-1	8.9797E-1	8.0191E-1	8.6299E-1	8.8842E-1	2.1763E0	4.0078E0
a_2	4.3665E-1	3.0569E-1	3.4568E-1	4.4104E-1	3.9381E-1	1.6571E0	1.1582E0
w_2	8.3890E-2	-9.8330E-2	1.2826E-1	8.1990E-2	1.1748E-1	-4.1520E-2	-1.7197E-1
δ_2	-1.2188E-1	-1.2136E-1	-1.2502E-1	-1.7386E-1	-1.7144E-1	-5.0374E-1	-9.8132E-1
RSS	5.6578E-6	4.5744E-6	3.4994E-6	3.2332E-6	2.4183E-6	3.0690E-6	3.7181E-7
$\chi^2_{\rm red}$	5.4930E-8	4.4412E-8	2.7995E-8	2.5865E-8	1.9347E-8	2.4552E-8	3.2903E-9

Continued on next page

Table 2 – continued from previous page

nucleus	^{104}Pd	^{106}Pd	^{108}Pd	^{110}Pd	^{144}Sm	^{148}Sm	^{150}Sm
R_1	5.0934E0	5.3621E0	5.2585E0	5.2737E0	5.5491E0	5.6729E0	5.6265E0
a_1	5.5269E-1	6.0421E-1	6.8224E-1	7.1975E-1	5.9683E-1	6.5125E-1	6.4832E-1
w_1	-4.8304E-1	-2.8731E-1	-1.6880E-1	-2.0479E-1	4.1067E-1	1.4591E-1	2.3409E-1
R_2	5.2701E0	1.0946E0	3.8203E0	4.2605E0	8.3251E-1	1.0900E-3	9.3559E-1
a_2	4.8023E-1	6.0453E-1	1.5504E0	1.3635E0	3.0813E-1	1.3865E0	2.7277E-1
w_2	-8.4770E-1	7.4208E-1	-1.3089E-1	-1.7141E-1	-6.5310E-2	1.1967E-7	-7.7434E-1
δ_2	-1.8471E0	-1.6475E-1	-4.2796E-1	-6.4328E-1	-3.2435E-1	-1.4875E0	-1.4004E-1
RSS	4.6030E-6	2.7584E-6	1.6377E-6	2.3784E-7	2.5702E-5	8.0769E-6	9.0084E-6
$\chi^2_{\rm red}$	4.0377E-8	2.4197E-8	1.4241E-8	2.0863E-9	2.7342E-7	8.5924E-8	9.5834E-8
nucleus	^{152}Sm	^{154}Sm	^{154}Gd	^{158}Gd	^{166}Er	^{174}Yb	^{175}Lu
R_1	5.9974E0	5.5482E0	6.2194E0	5.9738E0	6.2818E0	6.4931E0	6.0389E0
a_1	6.5237E-1	6.8418E-1	7.7116E-1	8.6817E-1	7.7104E-1	8.1193E-1	7.5439E-1
w_1	-2.3272E-1	4.0448E-1	-4.2260E-1	-3.8982E-1	-3.9660E-1	-5.4963E-1	-2.8040E-2
R_2	2.9424E0	1.6778E0	4.3203E0	5.0454E0	2.7188E0	4.0872E0	2.9883E0
a_2	3.6779E-1	3.3336E-1	4.9090E-1	6.1167E-1	8.0178E-1	1.1569E0	1.2036E0
w_2	1.5770E-2	2.4427E0	-9.6412E-1	-1.9423E0	7.9296E-1	-4.3770E-1	2.8464E-1
δ_2	-2.6086E-1	1.9731E-2	-3.9617E-1	-3.5530E-1	-4.6248E-1	-1.4630E0	-7.5172E-1
RSS	6.7970E-6	9.2795E-6	1.5187E-6	1.4602E-6	1.3384E-6	1.5457E-6	3.9738E-6
$\chi^2_{\rm red}$	7.9035E-8	8.5133E-8	1.4745E-8	1.3521E-8	1.1741E-8	1.3559E-8	3.4858E-8
nucleus	^{192}Os	^{196}Pt	^{204}Hg	^{203}Tl	^{205}Tl	^{204}Pb	^{206}Pb
R_1	6.3793E0	6.3358E0	6.4398E0	6.4524E0	6.4627E0	6.5664E0	6.5750E0
a_1	6.0052E-1	5.8907E-1	5.7421E-1	5.8354E-1	5.8302E-1	5.9014E-1	5.9754E-1
w_1	3.0380E-2	9.7160E-2	1.7490E-1	1.2865E-1	1.3554E-1	-7.3140E-2	-7.3030E-2
R_2	5.6120E-1	5.1668E-1	1.7066E0	8.1655E-1	1.4865E0	1.3681E-1	3.3280E-2
a_2	7.1657E-1	6.0430E-1	3.2251E-1	5.1228E-1	3.7563E-1	9.4296E-1	1.0056E0
w_2	3.4598E-1	3.7234E-1	8.3453E-1	6.9835E-1	3.4021E0	3.3980E-2	1.4000E-3
δ_2	-1.0167E-1	-9.5897E-2	-4.9042E-2	-6.6540E-2	-1.9804E-2	-1.4971E-1	-2.3444E-1
RSS	8.5973E-6	7.4914E-6	9.5724E-6	9.4721E-6	7.5945E-6	5.2925E-6	4.1066E-6
$\chi^2_{\rm red}$	7.5415E-8	5.9931E-8	7.6579E-8	7.5777E-8	6.0756E-8	4.2004E-8	3.2853E-8
nucleus	^{207}Pb	^{208}Pb	^{209}Bi				
R_1	6.5887E0	6.5774E0	6.5887E0				
a_1	5.9427E-1	5.9376E-1	5.8883E-1				
w_1	-8.7080E-2	-5.6310E-2	-3.3930E-2				
R_2	2.2544E-1	1.7500E-3	9.2030E-2				
a_2	9.2500E-1	9.5222E-1	8.8318E-1				
w_2	9.9640E-2	4.8401E-6	2.4960E-2				
δ_2	-1.4177E-1	-1.8946E-1	-1.0109E-1				
RSS	5.7246E-9	4.6261E-6	5.1785E-6				
$\chi^2_{\rm red}$	4.3368E-8	4.0939E-8	4.1428E-8				

together with the parameters obtained from fitting to model-independent density.

It is obvious that the 3pF function gives higher accuracy than 2pF function for the five nuclides presented in Table 1. For ^{60}Ni and ^{208}Pb, the improvement is slight compared to the improvement for the other nuclides. For ^{60}Ni, the RSS decreases only by 2% of its value when the depression parameter is considered. Thus, the fitted 2pF and 3pF distributions are almost identical for ^{60}Ni charge density. For ^{152}Sm, the RSS decreases by about 75% when the depression parameter is considered. This implies that the use of the 3pF distribution provides a significant improvement in the quality of the fit.

The fitting of model-independent density to the d3pF distribution provides a remarkable improvement over the other two formulae for the five nuclides considered in this study. For ^{40}Ca, ^{60}Ni, and ^{100}Mo, the RSS corresponding to d3pF is less than 1% of its values in the case of 2pF. For ^{152}Sm, and ^{208}Pb, the RSS is about 1.8% and 4.4%, respectively, of the corresponding values in the case of

2pF.

Table 2 presents the d3pF density distribution parameters, RSS and reduced chi-squared ($\chi^2_{\rm red}$) that have been obtained from the fitting of model-independent densities. The Fourier-Bessel coefficients from the data compilations of Vries et al [3] and Fricke et al [4] have been used to obtain the data of Table 2. For those nuclei which have several data sets, the most recent is considered. Some data sets do not obey the normalization condition and have unreasonable large central densities, in particular,^{90,92,94}Zr, ^{92}Z, ^{94,96,98,100}Mo, ^{198}Hg and ^{204,206,207,208}Pb in Ref. [4], and those nuclei are excluded from the present study.

4 Conclusions

The three formulae considered in this study provide a reasonable approximation of the charge, proton and neutron densities. From the statistical point of view, the fitting is improved as the number of adjustable parameters increase, but one should be careful when talking about the significance of improvement. For a calculation which is sensitive to the fine details of density, the improvement would be very significant. But for a calculation which deals only with the tail of density distribution, or where the fine details of core density does not affect the result, the improvement would be insignificant. Thus, consideration of the d3pF distribution would improve the calculation of nuclear structure and decay. In contrast, less improvement is expected for nuclear reactions and scattering calculations. The improvement in the different types of calculations should be studied carefully.

References

1 R. Hofstadter, Rev. Mod. Phys., **28**(3): 214-254 (1956)
2 C. W. Jager, H. De Vries, and C. De Vries, At. Data Nucl. Data Tables, **14**(5-6): 479-508 (1974)
3 H. Vries, C. W. De Jager, and C. De Vries, At. Data Nucl. Data Tables, **36**(3): 495-536 (1987)
4 G.Fricke et al, At. Data Nucl. Data Tables, **60**(2): 177-285 (1995)
5 J. D. Patterson, and R. J. Peterson, Nucl. Phys. A, **717**(3-4): 235-246 (2003)
6 L. L. Salcedo, E. Oset, M. J. Vicente-Vacas, and C. Garcia-Recio, Nucl. Phys. A, **484**(3-4): 557-592 (1988)
7 A. B. Jones, and B. A. Brown, Phys. Rev. C, **90**(6): 067304 (2014)
8 J. Liu, C. Zhang, Z. Z. Ren, and C. Xu, Chin. Phys. C, **40**(3): 034101 (2016)
9 H. Geissel et al, Phys. rev. lett., **88**(12): 122301 (2002)
10 R. K. Gupta, D. Singh, R. Kumar, and W. Greiner, J. Phys. G: Nucl. Part. Phys., **36**(7): 075104(2009)
11 M. Ismail, A. Y. Ellithi, A. Adel,and H. Anwer, Int. J. Mod. Phys. E, **25**(1): 1650004 (2016)
12 C. Wen, Y. P. Xu, D. Y. Pang, and Y. L. Ye, Chin. Phys. C, **41**(5): 054104 (2017)
13 W. M. Seif, and A. Abdurrahman, Chin. Phys. C, **42**(1): 014106 (2018)
14 M. Ismail, A. Y. Ellithi, A. Adel, and A. R. Abdulghany, J. Phys. G: Nucl. Part. Phys., **42**(7): 075108 (2015)
15 M. Ismail, A. Y. Ellithi, A. Adel, and A. R. Abdulghany, Nucl. Phys. A, **947**: 64-75 (2016)
16 P. G. Reinhard, J. Friedrich, and N. Voegler, Zeitschrift für Physik A Atoms and Nuclei, **316**(2): 207-212 (1984)
17 J. Dechargé, and D. Gogny, Phys. Rev. C, **21**(4): 1568 (1980)
18 M. Bender, P. H. Heenen, and P. G. Reinhard, Rev. Mod. Phys., **75**(1): 121-180 (2003)